Pulse Bifurcations and Instabilities in an Excitable Medium: Computations in Finite Ring Domains

M. Or-Guil[1], J. Krishnan[2], I. G. Kevrekidis[2], M. Bär[1]

[1]Max Planck Institute for the Physics of Complex Systems,
Nöthnitzer Straße 38, 01187 Dresden, Germany
[2]Department of Chemical Engineering, Princeton University,
Princeton, NJ 08544, U.S.A.

(February 8, 2008)

We investigate the instabilities and bifurcations of traveling pulses in a model excitable medium; in particular we discuss three different scenarios for the loss of stability *resp.* the disappearance of stable pulses. In numerical simulations beyond the instabilities we observe replication of pulses ("backfiring") resulting in complex periodic or spatiotemporally chaotic dynamics as well as modulated traveling pulses. We approximate the linear stability of traveling pulses through computations in a finite albeit large domain with periodic boundary conditions. The critical eigenmodes at the onset of the instabilities are related to the resulting spatiotemporal dynamics and "act" upon the back of the pulses. The first scenario has been analyzed earlier [M. G. Zimmermann *et al.*, Physica D **110**, 92 (1997)] for high excitability *resp.* low excitation threshold: it involves the collision of a stable pulse branch with an unstable pulse branch in a so called T-point. In the frame of traveling wave ordinary differential equations, pulses correspond to homoclinic orbits and the T-point to a double heteroclinic loop. We investigate this transition for a pulse in a domain with finite length and periodic boundary conditions. Numerical evidence of the proximity of the infinite-domain T-point in this setup appears in the form of two saddle-node bifurcations. Alternatively, for intermediate excitation threshold, an entire cascade of saddle-nodes causing a "spiraling" of the pulse branch appears near the parameter values corresponding to the infinite domain T-point. Backfiring appears at the first saddle-node bifurcation, which limits the existence region of stable pulses. The third case found in the model for large excitation threshold is an oscillatory instability giving rise to "breathing", traveling pulses which periodically vary in width and speed.

PACS numbers: 03.40.Kf, 47.54.+r, 82.40.Ck

I. INTRODUCTION

One-dimensional excitable media exhibit nonlinear traveling waves such as wave trains and solitary pulses. Examples include concentration waves in chemical reactions in solution and on surfaces [1–3], signal propagation in neurons and in cardiac tissue [4]. These processes are often modelled by reaction-diffusion (RD) equations of activator-inhibitor type [4,5]. A pulse is a localized structure; it may result from a finite amplitude perturbation of a linearly stable rest state. The pulse shape usually decays exponentially as a function of the distance from the pulse center. Pulses can be analytically approximated in the asymptotic limit where the dynamics of the activator is much faster than that of the inhibitor variable, and where the activator variable diffuses, but the inhibitor does not. There, it can be shown that a pulse exists and is stable [5].

More recently, spatiotemporal chaos has been found in a variety of excitable model systems. Several examples have been reported in models whose kinetics possess three distinct homogeneous steady states (fixed points); apart from the stable rest state, these media also exhibit two unstable fixed points [6–8]. One example arises in a model for catalytic CO oxidation, where the inhibitor is a so-called surface structure variable; its kinetic nullcline displays a sigmoidal shape - threshold dependence on the activator variable (adsorbate coverage) [9]. In contrast to the standard linear dependence of the inhibitor nullcline on the activator, this functional form leads to the additional fixed points mentioned above. Similar behavior is often seen in models in physiology describing the dynamics of the membrane voltage (activator) controlled by so called gating variables for the ion channels (inhibitor). The kinetics of these gating variables display again a threshold-type, sigmoidal dependence on the membrane voltage, often leading to three (spatially homogeneous) fixed points for the PDE [4]. If only a single gating variable is involved, these models are qualitatively similar to the equations for catalytic CO oxidation studied here; a good example is provided by the Morris-Lecar model used to describe the membrane potential in a barnacle muscle fiber [10].

If the inhibitor kinetics are fast enough, the CO oxidation model displays an instability that has been colloquially named backfiring of pulses [6]. Related phenomena include the wave-induced chemical chaos found in the Gray-Scott model for an autocatalytic chemical reaction [7], as well as complex behavior in amplitude equations describing dynamics near a Takens-Bogdanov

(TB) point [8]. In addition, even reaction-diffusion media whose kinetics are characterized by a single fixed point, sometimes display pulse instabilities and backfiring under excitable conditions [11,12]. An analysis of the traveling wave ordinary differential equations derived from the original PDEs for the CO oxidation model reveals the basic mechanism for the destruction of stable pulses leading to complex behavior: it involves a so-called T-point [13] as well as a rich web of bifurcations of pulse solutions [14]. More recently, a similar bifurcation structure has been found in a model for intracellular calcium waves in pancreatic acinar cells [15] and in the ultrarefractory version of the FitzHugh-Nagumo model [16]. The resulting complex dynamics is often governed by a coherent structure described as a "wave emitting front" [13], a nonlinear front involving a spatially uniform *unstable* state that invades a spatially uniform stable one. The unstable state behind the propagating front evolves into spatiotemporal chaos. Similar behavior has been seen in the amplitude equations in the neighborhood of the TB point, and was named "chaotic nucleation" by those authors [8].

In this paper we investigate instabilities and bifurcations in a model of a catalytic surface reaction [9]. Using a computer-assisted approach we calculate solution branches in large, finite domains, under periodic boundary conditions (which we will, with slight abuse of terminology, refer to as pulses) and perform linear stability analysis of these pulse solutions. The eigenvalues of the corresponding Jacobian reflect the growth exponents of perturbation modes. The emphasis of the present paper is on the form of the spectra and in particular on the shape of the critical modes; this is in contrast to earlier work which focused mostly on the pulse bifurcation structure [13,14].

A homogeneous steady state of reaction-diffusion equations in an infinite system possesses a continuous spectrum, reflecting the growth rates of perturbation modes. The eigenmodes are harmonic functions, whose wavenumber parametrizes the corresponding eigenvalues. In a very long or infinite system, a single pulse can conceivably be considered (in the appropriate norm) as a perturbation of this uniform solution. Under these circumstances, the modes far away from the pulse are still delocalized, harmonic wave modes; the continuous spectrum remains essentially unchanged. Furthermore, additional perturbation modes exist that are localized at the site of the pulse and decay exponentially away from it. The corresponding eigenvalues are discrete, in contrast to the continuous band of eigenvalues belonging to the nonlocalized modes. In infinite or periodic systems, the Goldstone mode is an example of such a localized mode. In a spatially homogeneous system it is given by the spatial derivative of the pulse profile, and accounts for a shift in space (due to translational invariance); the corresponding eigenvalue is zero.

A bifurcation or instability of a given solution upon change of a single control parameter is typically accompanied by a single real eigenvalue or a pair of complex

conjugate eigenvalues crossing the imaginary axis. For a real eigenvalue, a saddle-node bifurcation is the most common case, while alternative bifurcations like the transcritical or pitchfork bifurcations require certain symmetries for the equations and the solution. The case of a drift pitchfork bifurcation of a stationary pulse was studied in [17]. A destabilizing perturbation grows in an oscillatory manner if the eigenvalues are complex and in a non-oscillatory manner if the corresponding eigenvalue is real. The first case leads to a Hopf bifurcation, while the latter case may correspond either to a saddle-node or to a transcritical or pitchfork bifurcation.

Three examples of dynamics where localized initial conditions beyond the uniform solution excitation threshold do *not* eventually evolve into stable pulses, are shown in Fig. 1. For high excitability *resp.* small excitation threshold, pulse-like initial conditions evolve in a traveling pulse that splits off new pulse-like excitations traveling in the opposite direction. This is the phenomenon termed backfiring in [6]. It can eventually evolve in spatiotemporally chaotic (I) or complex periodic (II) fashion. For large excitation threshold, modulated traveling pulses are also seen (III). Their shape undergoes a breathing, periodic variation.
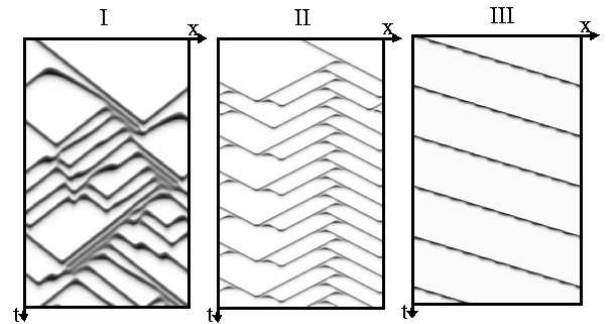

FIG. 1. Space-time plots from numerical integration of Eqs. (1) showing the time evolution of pulses at parameter values beyond the instability onset. A stable pulse solution for a subcritical parameter value, characterized by rest state A, was used as the initial condition. I: Backfiring in the immediate vicinity of a T-point. The resulting behavior is non-periodic for the given system length and initial conditions. II: Backfiring after a saddle-node bifurcation. The resulting behavior is periodic in time for the given system length and initial conditions. III: A supercritical Hopf bifurcation leads to modulated traveling waves. The pulse shows a periodic oscillation of shape and speed; variations appear mainly at its trailing edge. Black denotes high values of u, white corresponds to $u = 0$. Parameters: I: $b = 0.07$, $\epsilon = 0.1075, L = 100$, $\Delta T = 119.2$, II: $b = 0.15$, $\epsilon = 0.0931$, $L = 100$, $\Delta T = 238.42$, III: $b = 0.2$, $\epsilon = 0.062$, , $L = 50$, total integration time $\Delta T = 238.42$.

II. MODEL AND METHODS

We investigate a model of activator-inhibitor type originally derived for CO oxidation on Pt(110) [9], in a parameter regime where the kinetics give rise to one stable and two unstable steady homogeneous solutions. This model is related to the FitzHugh-Nagumo system and describes the interaction of a fast activator u and a slow inhibitor variable v:

$$\partial_t u = \partial_x^2 u + \frac{1}{\epsilon}u(1-u)(u - \frac{b+v}{a}),$$
$$\partial_t v = f(u) - v,$$

$$f(u) = \begin{cases} 0, & 0 \leq u < 1/3 \\ 1 - 6.75u(u-1)^2, & 1/3 \leq u \leq 1, \\ 1, & 1 < u \end{cases}$$

with $x \in [0, L]$ and periodic boundary conditions.

The time scales ratio $\epsilon > 0$ is used as the control parameter. The case $\epsilon \to 0$ corresponds to the aforementioned asymptotic limit where stable pulses are expected. The parameter b controls the excitability threshold of the system: the value of b is proportional to the magnitude of the critical perturbation which will trigger a pulse. The value of a is fixed at 0.84 throughout the paper. We will vary b, thus varying the excitability. In the parameter range considered here, three relevant fixed points exist: the stable state $A = (0, 0)$, the saddle $B = (b/a, 0)$, and unstable focus C.

We shall now examine the stability of pulses traveling in a background of the stable rest state A. Since we investigate solutions moving with fixed velocity c, the analysis of their stability is performed in the comoving frame $z := x - ct$:

$$\partial_t u = \partial_z^2 u + c\partial_z u + \frac{1}{\epsilon}u(1-u)(u - \frac{b+v}{a}),$$
$$\partial_t v = c\partial_z v + f(u) - v.$$

In this frame, traveling waves with speed c correspond to time independent, steady solutions. Linearization of these equations around a stationary solution $u_0(z), v_0(z)$ yields an eigenvalue problem for small perturbations $(r(z, t), s(z, t)) \propto (r(z), s(z))e^{\lambda t}$:

$$\mathcal{M} \begin{pmatrix} r(z) \\ s(z) \end{pmatrix} = \lambda \begin{pmatrix} r(z) \\ s(z) \end{pmatrix},$$

$$\mathcal{M} = \begin{pmatrix} \partial_z^2 + c\partial_z + g_1(z) & g_2(z) \\ \partial_u f(u_0) & c\partial_z - 1 \end{pmatrix}$$

with

$$g_1(z) = -\frac{1}{\epsilon}\left(u_0(u_0 - 1) + (u_0 - \frac{b+v_0}{a})(2u_0 - 1)\right),$$
$$g_2(z) = \frac{u_0}{\epsilon a}(u_0 - 1).$$

The linear stability problem amounts to the determination of the spectrum of the Jacobian $\mathcal{M}$ in (3). For the

homogeneous steady states A or B, at least one of the off-diagonal matrix elements is zero. Thus, the diagonal elements of the matrix $\mathcal{M}$ suffice to compute the spectrum. For the A steady state it is:

$$\lambda_{A,1} = -\frac{b}{\epsilon a} - k^2 + ick, \quad \lambda_{A,2} = -1 + ick, \qquad (4)$$

and for the B steady state it is:

$$\lambda_{B,1} = -\frac{b}{\epsilon a}\left(\frac{b}{a} - 1\right) - k^2 + ick, \quad \lambda_{B,2} = -1 + ick, \qquad (5)$$

where k is the wavenumber of the perturbation. In the case of periodic boundary conditions studied here, $k = n\frac{2\pi}{L}$ applies. The real part of the eigenvalues λ_2 is -1. The eigenvectors are then $(r, s)^T = (1, 0)^T e^{ikz}$ and $(0, 1)^T e^{ikz}$.

In general, traveling wave solutions $u_0(z), v_0(z)$ and the eigenfunctions of the Jacobian $\mathcal{M}$ are not available in closed form. Thus, the problem has to be approximated numerically. We approximate pulses by computing steady solutions in a finite length system and the traveling frame through a pseudospectral discretization of Eqs. (2) with periodic boundary conditions and Newton-Raphson iterations. The velocity c, which is not known *a priori*, is formally an additional variable along with the Fourier coefficients of the solution. One additional pinning condition singles out one of the infinitely many solutions existing due to translational invariance and allows the numerical computation of the speed. The eigenfunctions and the spectrum of the Jacobian are obtained in Fourier space resulting from a 200 (*resp.* 250 for case I) mode decomposition of the stationary solution. The zero eigenvalue, which always exists due to the translational symmetry of the problem, is used as a numerical accuracy check and has been obtained with a precision of 10^{-3} or better. The time evolution of unstable solutions was computed using an explicit finite difference scheme to solve Eqs. (1), discretizing space in 1024 points and using a time step of $\Delta t = 0.0122$.

Because traveling solutions fulfill the conditions $\partial_t u = \partial_t v = 0$ in the comoving frame, they can also be obtained in the traveling wave ordinary differential equations (TWODE) following from Eqs. (2):

$$\frac{du}{dz} = w,$$
$$\frac{dw}{dz} = -cw + \frac{1}{\epsilon}u(u-1)(u-u_{th}),$$
$$\frac{dv}{dz} = (v - f(u))/c,$$

with $u_{th} = (b+v)/a$. In this frame, a homogeneous solution corresponds to a fixed point, a pulse to a homoclinic orbit, and a front to a heteroclinic orbit. Consequently, in the parameter range studied here, three relevant fixed

3

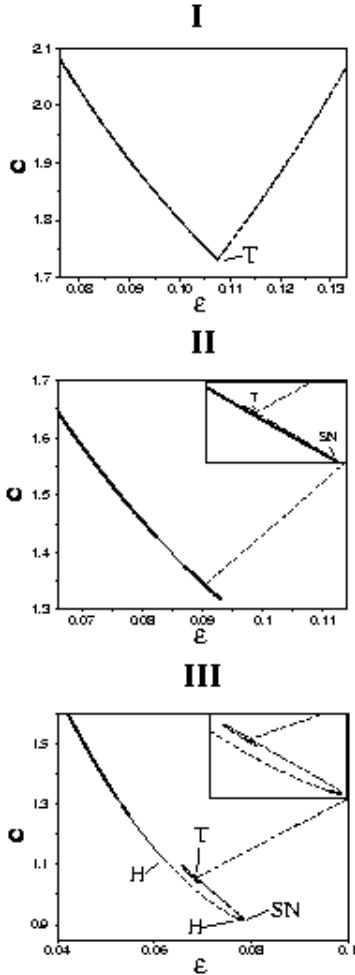points exist: $\mathcal{A} = (0,0,0)$, $\mathcal{B} = (b/a, 0, 0)$, and the focus C.

FIG. 2. Pulse speed as a function of the parameter ϵ. I: $b = 0.07$, II: $b = 0.15$, and III: $b = 0.2$. Thick lines are pulses with rest state A (i.e. pulses in a large box with periodic boundaries representative of pulses to the state A on the infinite line corresponding to the homoclinic orbits to $\mathcal{A}$); thin lines are pulses with rest state B. Solid (dashed) lines denote stable (unstable) branches. A T marks our approximation of the double heteroclinic connection point (the T-point) where pulses with rest state A "collide" with pulses with rest state B. H denotes Hopf bifurcations, SN denotes saddle-node bifurcations. In the cases II and III, the branch of pulses with rest state A spirals into the T-point. This is not the case for I, compare Fig. 3b.

III. RESULTS

We consider three cases, at increasing values of the excitation threshold, controlled through the parameter b at fixed $a = 0.84$: Case I ($b = 0.07$), case II ($b = 0.15$) and case III ($b = 0.20$). We proceed as follows: first, branches of pulse solutions on a ring, representative of ,,true" pulse solutions in a infinite domain, are presented for the relevant range of the control parameter ϵ; we characterize these pulses by their speed c (Fig. 2, 3b). We then show pulse profiles and spectra at selected values of ϵ shortly before and after the onset of instability (Figs. 3, 7, 8), and present the destabilizing mode $(r, s)^T$ (Figs. 6, 7, 8). Representative post-instability spatiotemporal dynamics can be found in Fig. 1.

Fig. 2 shows pulse speed as a function of the parameter ϵ for the three cases. The thick lines correspond to stable pulses with background state A, while dashed lines correspond to unstable pulses with background state B. The transition point between the two families is the so called T-point [23], denoted by a T. This point is defined as a double heteroclinic connection between the fixed points A and B in the frame of the traveling wave ODEs, Eqs. (6). In the frame of the original equation (1), these heteroclinic orbits correspond to fronts. The branch of pulses corresponding to homoclinic orbits to $\mathcal{A}$ in the TWODE may (Fig. 2.II, III) or may not (Fig. 2.I) spiral into the T-point. Spiraling is observed when two of the eigenvalues of the linearization of the TWODE around the fixed point $\mathcal{B}$ are complex conjugate [13].

A. Case I

Fig. 2.I shows speed as a function of the parameter ϵ for $b = 0.07$ computed for pulses in a large system with periodic boundaries. The picture appears at first glance identical with the result found in a continuation of homoclinic orbits in the TWODE [13]. The branch of pulses to A (thick line) does not spiral into the T-point. To be exact, the T-point only exists for pulses on the infinite line; what – at the resolution of our picture – still appears as a T-point will be discussed in more detail below. To understand the nature of the instability in this case, we focus on the solutions near the T-point value $\epsilon_T \approx 0.10744$.

As mentioned above, for an infinite system, the T-point corresponds to a double heteroclinic connection in the traveling wave ODEs, Eqs. (6). Close to ϵ_T the orbits homoclinic to $\mathcal{A}$ also approach the fixed point $\mathcal{B}$ (and vice versa); this approach to $\mathcal{B}$ makes the dynamics in z progressively slower. Thus, close to ϵ_T, pulses with rest state A (resp. B) will also exhibit extensive regions close to B (resp. A), practically giving rise to *fronts* between A and B within the pulse profile. When we perform a continuation *for a pulse in a ring of finite length*, the space on the ring is apart from the excitation plateau divided between residence close to A and residence close to B, so that the total period is constant as we vary ϵ.
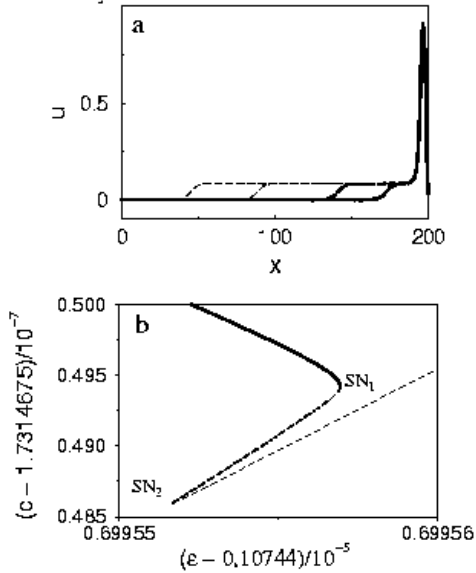
4

FIG. 3. a) Four pulse solutions on the ring from the middle branch in (b) illustrating the gradual transformation from solutions identifiable with pulses with rest state A ($u = 0$) to unstable solutions identifiable with pulses with rest state B ($u = 0.083$). The B domain in the waveform becomes wider upon decrease of ϵ, along the middle branch in (b). b) Bifurcation diagram, with respect to ϵ, of pulses for case I, exhibiting two saddle-nodes. The thick solid line can be associated with stable pulses homoclinic to A; the thin dashed line can be associated with unstable pulses homoclinic to B. The thick dashed line corresponds to the transition region between these two cases; it constitutes the incarnation (for our finite, large ringlength continuation) of the T-point. When the upper saddle-node bifurcation (SN_1) takes place, our finite ringlength solution could be still described as an approximation of a pulse to A but with a small B shoulder; the converse description holds at the lower saddle-node bifurcation (SN_2). It is reasonable to consider as most representative of the infinite-domain T-point the location, along this thick-dashed line, where the pulse solution contains comparable large patches close to A and close to B – roughly the middle of this middle-branch.

To study this behavior, numerical continuation techniques are needed. We computed the stationary solutions of Eqs. (2) on a ring of length $L = 200$ with 250 modes, 1024 collocation points and a parameter step size $\Delta\epsilon = \mathcal{O}(10^{-10})$. Periodic approximations of pulse solutions with rest state A are shown in Fig. 3a as they approach the T-point and undergo the gradual transition to pulse solutions with rest state B. One can clearly recognize the increasing domain $B = (b/a, 0)$ at the back of the pulse. As the state B is unstable, one might expect that the pulse in the ring loses stability as soon as the B domain gets large enough. However, one should be aware of the fact that the B domain is moving with the speed of the pulse. It is possible that the B domain is only convectively unstable in the comoving frame. In other words,

the perturbations growing on the B state in a stationary frame may spread slower than the pulse motion, and the pulse in an infinite domain will be stable. A mathematically precise description of this phenomenon has been given by Sandstede and Scheel [19]. A related result has been obtained by Nii [20], who shows that eigenvalues accumulate in the area bounded by the essential spectra of A and B. The opposite case, *i.e.* perturbations on the B plateau spread faster than the pulse speed, is described in the next subsection (case II).

Typical spectra are shown in Fig. 4 for solutions along the $c - \epsilon$-branch. To facilitate a better comparison, the continuous spectra of the rest states A (Eqs. (4)) and B (Eqs. (5)) are depicted as solid lines; the computed eigenvalues are denoted by circles. Fig. 4a shows the spectrum of a solution approximating a stable pulse with rest state A, while Fig. 4f shows that of a solution approximating an unstable pulse with rest state B. In both cases, the parameter ϵ is "far" from the T-point bifurcation and the eigenvalues belonging to nonlocalized eigenvectors compare well with the continuous spectrum of the respective rest state. Figs. 4b-e show the gradual transition between the two cases. Fig. 4b shows the spectrum for a stable solution for which the domain B is just starting to appear in the back of the pulse. Its width is $L_B \approx 5$. Several discrete eigenvalues have appeared on the negative real axis; a similar spectrum has been predicted and found by Sandstede and Scheel [19].

The details of the spectrum tranformation are as follows: Initially (far to the left of the T-point in Fig. 2a), the pulse spectrum contains two discrete complex conjugate eigenvalues (which remain more or less unchanged through the bifurcation diagram) as well as two "pieces" of continuous spectrum: a parabola, and a vertical line. For our calculations in the finite domain, initially the parabola *does* have a "tip" (an eigenvalue on the real axis) while the vertical line *does not* have an eigenvalue on the real axis. As we vary ϵ the parabola approaches the straight line; eventually the parabola appears as *crossing* the line. While this occurs, a number of complex conjugate pairs of eigenvalues emerge from the parabola and line approximating the essential spectrum. Fig. 4a shows the situation where the first of these pairs has appeared. Upon further increase of ϵ, these pairs collapse on the negative real axis where they split and become real. These real eigenvalues lie in the *absolute* spectrum of state B (see [19]); they appear when the solution has a visible B "shoulder" behind the pulse, see Fig. 4b. As ϵ varies these real eigenvalues become complex conjugate. Several complex eigenvalue pairs of the parabola give the appearance of a secondary parabola - this is the first intimation of what will become the essential spectrum of B. Only two of the "momentarily real" eigenvalues remain real - one of them forms the tip of the "new parabola", while the other forms the tip of the "old parabola".

Gradually, as the B plateau grows, two distinct phases of spectrum movement are observed. First this new B-associated parabola moves to the right in the complex

plane and at some point it starts crossing the imaginary axis. That is precisely the first saddle-node bifurcation we observe - the critical eigenvalue is the tip of this secondary parabola, whose origin we just discussed, see Fig. 4c. Continuing further on the middle, already unstable branch, the B-domain gets wider and many secondary (apparently Hopf) bifurcations occur as the eigenvalues of this "discretized" parabola cross successively the imaginary axis. When both A- and B-plateaus are equally present, one expects to see echoes of both A- and B-continuous spectra in the solution spectrum, and that is indeed seen in Fig. 4d. Near the lower saddle-node bifurcation, the B-plateau is almost as wide as the system length. There, one may describe the solution more reasonably as an approximation to a pulse with rest state B with a short A domain at its front. The eigenvalue spectrum at this situation is depicted in Fig. 4e. The second (lower) turning point occurs when the "discretized" parabola of eigenvalues that corresponded initially to continuous spectrum of A moves to the right and the real eigenvalue at the tip of this discretized parabola crosses the imaginary axis.
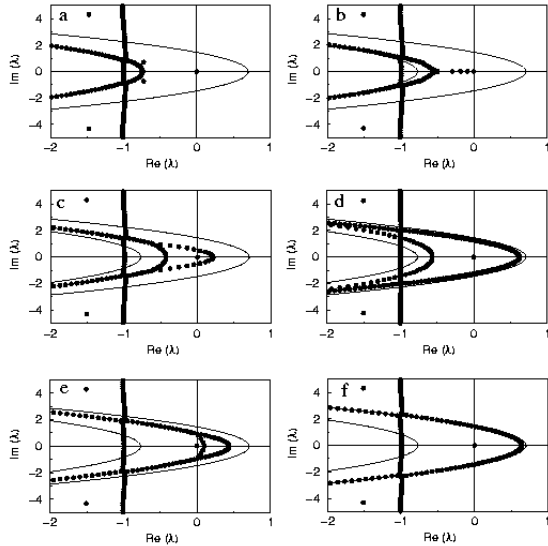

FIG. 4. Spectra of pulses in case I for different values of ϵ. The solid lines correspond to the continuous spectrum of the rest state A, Eqs. 4 (left parabola) resp. rest state B (right parabola), Eqs. 5. The pictures show the typical change of the spectrum along the solution branch c-ϵ. Parameters: $a = 0.84$, $b = 0.07$, $L = 200$ ($L = 400$ for picture d), a) $\epsilon = 0.106425824$, b) $\epsilon = 0.107446965$, c) $\epsilon = 0.107446995547$, d) $\epsilon = 0.1079$, e) $\epsilon = 0.107446995527$, f) $\epsilon = 0.109936154$.

Eventually, the old A-parabola eigenvalues merge with the B-parabola as the A-shoulder gradually disappears. Fig. 4f shows the spectrum for a solution approximating a pulse with rest state B far from the T-point bifurcation for a high values of ϵ. In the end, the two "tips" (the old and the new one) collide and become again a complex conjugate pair - the final pure-B parabola has no real tip.

Sandstede and Scheel in [19] have proven that the spectrum of pulses with rest state A with a "shoulder" of B state as in Fig. 3a is comprised of the essential spectrum of the homogeneous background state A plus eigenvalues lying in the absolute spectrum [21] of B located on the real axis and bounded by a maximum value which is negative. We deviate from their picture, when the B shoulder becomes relatively large. In other words, their result on the infinite line is reproduced by our numerical stability analysis in the ring, if the condition $L_B << L$ holds. The spectrum transformations, however, reflect the influence of the periodic boundary conditions and the finite length. Because of the violation of the above assumption near the T-point (see Fig. 3a) the spectra we find for a large box are not well described as the union of the essential spectrum of A and the absolute spectrum of B. The results of [19] also imply that if one considers pulses on the infinite line instead of the large wavelength approximation with periodic boundary conditions used here, one will find a monotonic approach of the pulse branches to the T-point. In their scenario no eigenvalues are crossing the real axis upon approaching the T-point (in contrast to the computations on the ring) and no bifurcation (like the saddle-node bifurcation found for the ring) can occur.

Focusing on the first instability (SN_1), the critical eigenmode corresponding to the saddle-node appears localized at the back of the pulse (see Fig. 5). In addition, it is acting mainly on the activator (Fig. 5b); we observe that new pulses can now split off the existing pulse ("backfiring"). Fig. 6 shows the time evolution beyond the saddle-node bifurcation in a comoving frame. The initial condition is the stable pulse just before the bifurcation. Fig. 6a shows how a perturbation with support over the B-plateau grows with time, while the shape of the preceding front essentially does not change. The back (what starts as the B-plateau) grows until its maximum reaches the excited state $u = 1$. The excited domain widens, but its plateau is unstable against oscillating perturbations [13]. Therefore, the situation rapidly evolves, and the growing excited domain breaks down, giving rise to two new seeds for A-pulse like entities. This behavior has been described by the term "backfiring" [6,13]. Backfiring occurs repeatedly, and the newly generated pulse-like structures annihilate upon collision with similar objects traveling in the opposite direction; this interplay of instability, new pulse generation and annihilation gives rise to the non-periodic space-time behavior shown in Fig. 1.I.
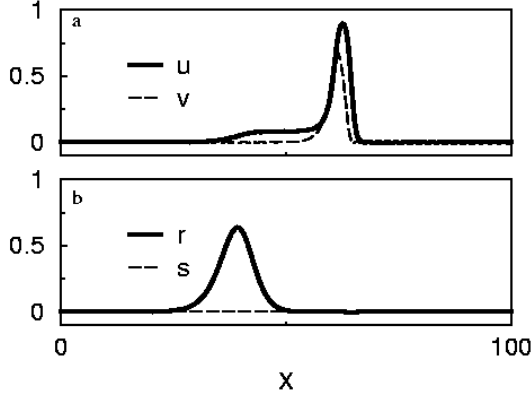
6

FIG. 5. a) Unstable pulse solution in case I in the vicinity of the saddle-node bifurcation SN_1, Fig. 3b. b) Destabilizing eigenmode. Parameters: $a = 0.84$, $b = 0.07$, $\epsilon = 0.1074469956$, $L = 200$. Only part of the domain is shown.
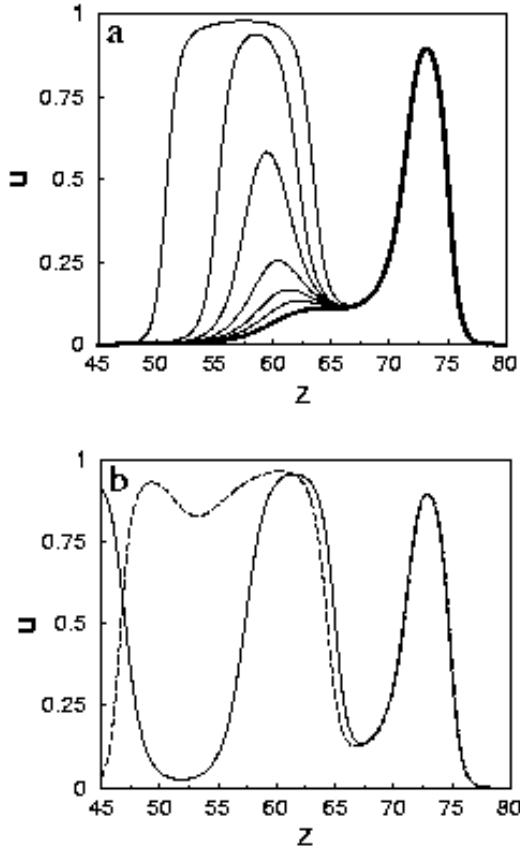

FIG. 6. Time evolution for a value of ϵ after the saddle-node bifurcation SN_1 in a comoving frame. The initial condition is the stable pulse-like solution just before the bifurcation (thick black line in a)). The thin lines in a) demonstrate how the shape of the solution changes only at the back of the pulse-like solution. A localized perturbation grows in amplitude and width in the course of time and approaches the rest state C, where $u = 1$. Further evolution of the dynamics is given by the dashed line in picture b). Due to oscillatory instability of the homogeneous state C, the corresponding domain cannot become large. A breakdown leads to the generation of two further pulse-like states traveling in opposite directions (thin solid line).

Altogether, our results give an interesting and well resolved picture of stability of pulses on a large finite ring near the T-point. In contrast, earlier computations [13,14] have used coarser steps in the continuation algorithms and smaller domains. The present computations show how the pulse solutions change in a gradual fashion; and that two distinct solutions branches show an extremely narrow hysteresis; the middle branch mediates the transition between the two different pulse types. The main changes appear in an extremely tiny region of parameter space and can therefore only be captured with careful numerics. The spectrum transformations near parameters that exhibit a T-point in the corresponding TWODE appear in a similar fashion for case II and III studied below. There, however, the T-point is not involved in the disappearance of stable traveling pulses through instability and bifurcation. Thus, we will not discuss it in these cases.

B. Case II

Fig. 2.II shows the $c - \epsilon$ diagram for $b = 0.15$. As in case I, we again observe here the transformation from pulses with rest state A to pulses with rest state B at what appears like a T-point. The branch corresponding to "pulses to A" spirals into this T-point. This behavior is caused by imaginary eigenvalues of the fixed point B in the TWODE at the T-point conditions, and has been predicted from general arguments [23]. Thus, the branch of initially stable pulses with rest state A undergoes a sequence of saddle-node bifurcations upon approaching the T-point. This sequence of saddle-node bifurcation is consistent with the results of Sandstede and Scheel [19]. The spectrum of A-pulses near the T-point in the infinite system approaches the union of the essential spectrum of A and the absolute spectrum of B. In this case, however, the absolute spectrum of B contains real *positive* eigenvalues. One may, therefore expect infinitely many saddle-node bifurcations as the T-point is approached. In the stability-relevant first saddle-node bifurcation, the solution branch of stable wavetrains with rest state A turns around and becomes unstable. As is required for a saddle-node bifurcation, a single real eigenvalue crosses

the imaginary axis. This can be seen in Fig. 7, left column. The two spectra correspond to pulse-like solutions before and after the saddle-node bifurcation along the solution branch. The unstable pulse and the destabilizing eigenmode are shown in Fig. 7, right column. Once more, the destabilizing mode affects primarily the back of the pulse. It is worth noting, that upon further continuation the branch of pulses to A spirals towards the T-point related situation over a cascade of saddle-node bifurcations. Each saddle-node bifurcations adds an additional positive eigenvalue to the spectrum. This is in contrast to the study in [24], where a single eigenvalue repeatedly crosses zero along a spiraling pulse branch with a cascade of saddle-node bifurcation.
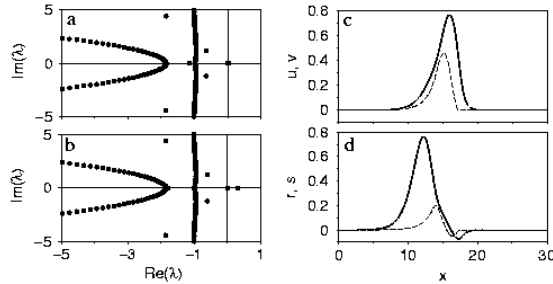

FIG. 7. Case II: a) Eigenvalues at $\epsilon = 0.0927$ before a saddle-node bifurcation of a pulse decaying into the rest state A; b) eigenvalues at $\epsilon = 0.09299$ after this bifurcation. A discrete eigenvalue crosses the imaginary axis. c) Unstable solution and d) corresponding destabilizing eigenmode $(r, S)^T$ at $\epsilon = 0.09299$. Parameter: $a = 0.84$, $b = 0.15$, $L = 100$.

Numerical simulations of the model Eqs. 1 shortly after the saddle-node bifurcation, for values of ϵ for which no solution with rest state A exists, exhibits the phenomenon we termed above "backfiring". In the transients, our pulse-like object generates near its back other pulse-like entities traveling in the opposite direction, see Fig. 1.II. After this transient period, the resulting spatiotemporal pattern in our finite domain becomes periodic in time. Simulations show, though, that this observation depends on the initial conditions: non-periodic patterns like the one shown in Fig. 1.I may also appear for the same parameter values.

C. Case III

Fig. 2.III shows the $c - \epsilon$ 0 for $b = 0.2$. Here, the pulse solution with rest state A becomes unstable through a Hopf bifurcation even before the first saddle-node bifurcation is reached. The eigenvalue spectrum is shown in Fig. 8, left column, on both sides of this Hopf bifurcation. It can be seen that one discrete pair of complex conjugate eigenvalues crosses the imaginary axis. The second column of Fig. 8 shows the pulse-like solution *after* the

bifurcation as well as the real and imaginary parts of the critical eigenmode $(r, s)^T$. Note that the perturbation due to the eigenmode is localized and has its main contribution – once more – at the back of the pulse. As the corresponding eigenvalues are complex conjugate, the resulting perturbation oscillates with time at a frequency given by the imaginary part of the eigenvalues.
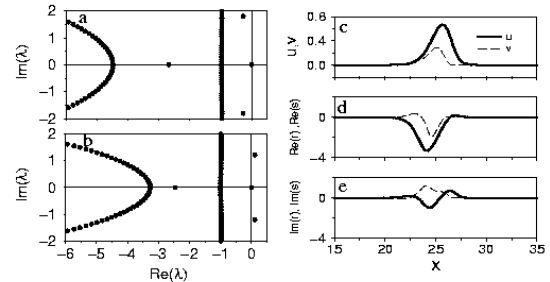

FIG. 8. Case III: a) Eigenvalues at $\epsilon = 0.053$ before a Hopf bifurcation; b) eigenvalues at $\epsilon = 0.072$ after this bifurcation. A discrete pair of complex conjugated eigenvalues crosses the imaginary axis. c) Unstable pulse-like solution as well as d) real and e) imaginary part of the corresponding destabilizing eigenmode $(r, s)^T$ at $\epsilon = 0.065$. Parameters: $a = 0.84$, $b = 0.2$, $L = 50$

Numerical integration of the model Eqs. (1) shows that the Hopf bifurcation which leads to destabilization is supercritical [14]. The resulting pattern after destabilization consists of a *modulated* traveling pulse which oscillates in time, especially at its back (compare the simulation shown in Fig. 1.III.)

IV. CONCLUSION

We have investigated the transition from stable pulse propagation to various regimes of more complicated spatiotemporal dynamics, namely modulated pulses, periodic and chaotic pulse backfiring. In all three cases, the transition can be explained by either a Hopf instability (modulated pulses) or a saddle-node bifurcation (leading to backfiring) of the stable pulse solution. In all cases, the transition is connected with either a single or a pair of complex conjugate discrete eigenvalue(s) with zero real part(s). In a finite domain with periodic boundary conditions – the typical experimental setup for investigation of pulses – spectra change continuously near the T-point in the fashion described in case I. The form of the corresponding critical eigenmode(s) allows some insight into how pulses become unstable *resp.* evolve in space and time. The dynamics in general still contains mostly propagating localized pulse-like structures whose evolution is governed by the unstable eigenmode(s) in the Hopf case (modulated) or by the critical eigenmode of the saddle-node bifurcation. Typically, the critical eigenmodes have support at the back of the pulse.

The results here should carry over to models with similar phenomenology mentioned in the introduction. Preliminary results [25] show that the transition to wave-induced chemical chaos in the Gray-Scott model [7] is also caused by a saddle-node bifurcation of pulses near a T-point. T-points can only be found in systems with multiple homogeneous fixed points (*e.g.* one stable rest state and two additional unstable steady states). The complex behavior seen in media with a single stable fixed point [11,12] may be caused through a different mechanism. For a model of the catalytic NO-CO reaction, upon change of control parameter first modulated traveling waves are seen and then periodic backfiring is found. This cannot be due to a T-point, but may instead be caused by a global bifurcation of the periodic modulated pulses - a scenario already suggested in a study of the present model with different control parameters [14]. Finally, it is important to note that a simple instability of a finite wavelength pulse solution, like the Hopf bifurcation in case III, only leads to a modulation of the shape, while a saddle-node bifurcation limits the existence of a certain type of pulses and may give rise to replication of pulse-like structures (cases I, II). The role of saddle-node bifurcations in the replication of pulses and creation of space-time defects has recently been investigated in the Gray-Scott model [26] and in the Complex-Ginzburg-Landau equation [27].

[1] J. Ross, S. C. Müller, and C. Vidal, Science, **240**, 466 (1988).

[2] R. Kapral, and K. Showalter (Eds.), "Chemical Waves and Patterns", (Kluwer, Dordrecht, 1995).

[3] S. Jakubith, A. von Oertzen, H. H. Rotermund, and G. Ertl, Phys. Rev. Lett. **65**, 3013 (1990).

[4] J. Keener and J. Sneyd, *Mathematical Physiology* (Springer, New York, 1998).

[5] A. S. Mikhailov, *Foundations of Synergetics I*, (Springer Verlag, New York, 1990).

[6] M. Bär, M. Hildebrand, M. Eiswirth, M. Falcke, H. Engel and M. Neufeld, Chaos **4**, 499 (1994).

[7] J. H. Merkin, V. Petrov, S. K. Scott and K. Showalter, Phys. Rev. Lett. **76**, 546 (1996); J. Chem. Soc., Faraday Trans. **92**, 2911 (1996).

[8] M. Argentina and P. Coullet, Phys. Rev. E **56**, R23259 (1997).

[9] M. Bär, N. Gottschalk, M. Eiswirth, and G. Ertl, J. Chem. Phys. **100**, 1202 (1994).

[10] C. Morris and H. Lecar, Biophys. J. **35**, 193 (1981).

[11] M. Mimura and M. Nagayama, Chaos **7**, 817 (1997).

[12] J. Christoph and M. Eiswirth, unpublished results; see also M. Bär, R. Hegger and H. Kantz, Phys. Rev. E **59**, 337 (1999).

[13] M. G. Zimmermann, S. O. Firle, M. Natiello, M. Hildebrand, M. Eiswirth, M. Bär, A. K. Bangia, and I. G. Kevrekidis, Physica D **110**, 92 (1997).

[14] J. Krishnan, I. G. Kevrekidis, M. Or-Guil, M. G. Zimmermann, and M. Bär, Comp. Methods in Appl. Mech. and Eng. **170**:(3-4) 253 (1999)

[15] J. Sneyd, A. LeBeau and D. Yule, Physica D **145**, 158 (2000).

[16] M. M. Romeo and C. K. R. T. Jones, Phys. Rev. E **63**, 011904 (2001).

[17] M. Kness, L. Tuckerman and D. Barkley, Phys. Rev. A **46**, 5054 (1992).

[18] E. J. Doedel and X. J. Wang, AUTO 94: Software for continuation and bifurcation problems in ordinary differential equations, Technical report, Center of Research on Parallel Computing, California Institute of Technology, Pasadena, CA 911125, CRPC-95-2.

[19] B. Sandstede, and A. Scheel, Nonlinearity **13**, 1465 (2000).

[20] S. Nii, Physica D **142**, 70 (2000).

[21] The absolute spectrum is defined in [19]. For the example investigated here, the absolute spectrum of B at the T-point lies on the real line and is given by the interval $[-0.77564, -0.03847]$. For other parameters, the absolute spectra lies on the interval $[-\frac{b}{a\epsilon}, -\frac{c^2}{4} + \frac{b}{a\epsilon}(1 - \frac{b}{a})]$.

[22] B.Sandstede and A. Scheel, Physica D **145**, 233 (2000).

[23] P. Glendinning, and C. Sparrow, J. Stat. Phys. **43**, 479 (1986).

[24] H. C. Chang, E. A. Demekhin, D. I. Kopelevich, Physica D **97**, 353 (1996).

[25] M. Zimmermann, M. Or-Guil and M. Bär, unpublished results.

[26] Y. Nishiura and D. Ueyama, Physica D **130**, 73 (1999).

[27] L. Brusch, M. G. Zimmermann, M. van Hecke, M. Bär and A. Torcini, Phys. Rev. Lett. **85**, 86 (2000).